Observations of the Deepening of the Wind-Mixed Layer in the Northeast Pacific Ocean

DAVID HALPERN

Pacific Marine Environmental Laboratory/NOAA, University of Washington, Seattle 98195

(Manuscript received 4 December 1973, in revised form 13 February 1974)

ABSTRACT

Measurements of winds, currents and temperature are used to describe the response of the upper ocean in the northeast Pacific to the passage of an August 1971 synoptic-scale meteorological disturbance. The experiment was designed so that at the beginning of the 32-day study the uppermost two current meters were located in the upper isothermal layer, a third current meter was placed at the top of the seasonal thermocline, and the fourth current meter was located near the bottom of the seasonal thermocline. Thermistors attached to a multi-conductor cable were placed in the mixed layer and in the thermocline region.

Before the onset of the storm the thickness of the mixed layer was about 15 m. The storm produced a more homogeneous temperature distribution above 20 m with a lower average temperature, higher temperature values below 20 m, and a thicker (25 m) mixed layer. The heat content of the upper layer changed little ($<\pm 5\%$) as the mixed layer deepened. The storm generated large currents and vertical current shears, especially at the inertial frequency. Currents in the mixed layer were strongly coupled to the wind and responded to the large increase in the wind speed within a time interval equal to about a half-pendulum day; the currents in the stably stratified water beneath the mixed layer were weakly coupled to the storm.

During the experimental interval the water in the upper 50 m was, on the average, dynamically stable as measured by the Richardson number. After the onset of the storm the dynamic stability of the transition zone between the mixed layer and the stratified region was marginal ($\mathrm{Ri}<1$) for a period of a few days and vertical mixing was produced by the large velocity shear. The stratified region was always dynamically stable. Quantitative estimates of the mixing are discussed: the increase in the potential energy of the water column is compared to the amount of available mixing energy, and the depth of the mixed layer produced by the storm is compared with theoretical results and with other observations.

1. Introduction

As our knowledge of the variability of the motions within the ocean increases it becomes evident that one of the more significant factors determining the time-dependent behavior of the upper ocean is the large energy exchange occurring at the ocean-atmosphere boundary during the passage of storms. In a region away from oceanic boundaries and in the absence of turbulent mixing by strong currents, the thickness of the surface mixed layer is assumed to be influenced by two surface-induced processes, wind mixing (forced convection) and convective mixing (free convection). In wind mixing are included all the vertical turbulent mixing processes resulting initially from the transfer of momentum from the wind. Convective mixing occurs as a result of instability generated at the surface by surface cooling and by evaporation of fresh water from the sea. According to Niiler (1973) the erosion of a stably stratified, quiescent upper ocean layer is initially characterized by a rapid deepening, qualitatively predicted by Pollard *et al.* (1973), and a subsequent slow erosion, as parameterized by Denman (1973a) follows.

It is fairly well established that inertial oscillations observed in the surface mixed layer of the ocean are generated by local winds (Pollard and Millard, 1970; Sakou, 1970); furthermore, the amplitude of these motions appears to be discontinuous at the bottom of the mixed layer (Pollard, 1970). Webster (1972) has shown that these motions are weakly coupled to the smaller amplitude oscillations occurring in the stratified water beneath the mixed layer. Is the amplitude discontinuity sufficiently strong and the coupling sufficiently weak so that dynamic instabilities are generated in the transition zone between these two layers? And if so, is this a mechanism for the erosion of the thermocline (or increasing the depth of the mixed layer) and for the propagation of energy into the deeper regions of the ocean? In an attempt to answer these questions we conducted a 32-day experiment in the northeast Pacific between 4 August and 5 September, 1971. In this investigation the following parameters were measured from a surface float mooring: wind speed and direction, air and sea surface temperatures, and in the uppermost 55 m of the water column, the temperature at eight locations and the currents at four depths.

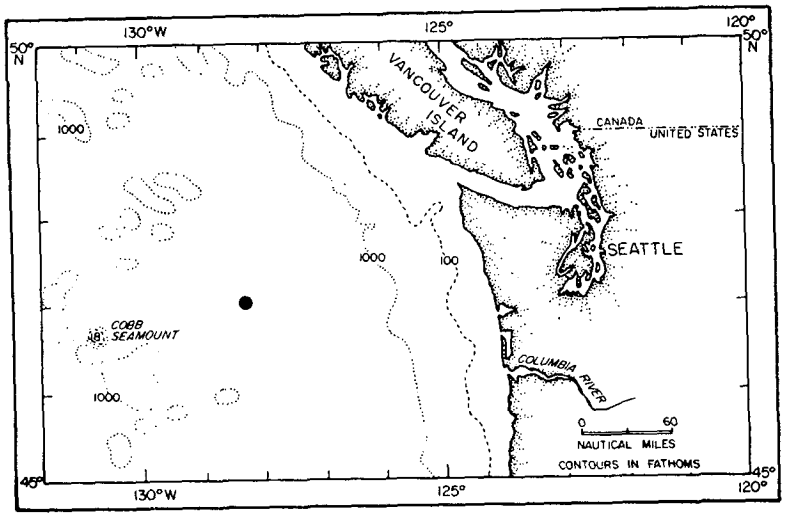

FIG. 1. Location of experimental site represented by black dot. Contours are in uncorrected fathoms.

The experimental site, which was located at approximately 47°03.4'N, 128°17.2'W, was about 250 km from the continental shelf break and about 220 km from Cobb Seamount of the Juan de Fuca Ridge (Fig. 1). This position, which had a water depth of about 2700 m, was chosen because of the absence of strong permanent-type currents and because it was a deep water region far from bathymetric or coastal features that might influence the wind-generated circulation of the uppermost 100 m. This area was also far from land so that the wind circulation was not influenced by terrestrial features. Uda's (1963) description of the mean circulation indicates that the buoy was located in the region of separation of the West Wind Drift where the surface baroclinic geostrophic currents (relative to 1000 m) were variable in direction and weak, less than 5 cm sec^{-1}.

2. Instrumentation

At the beginning of the experiment the uppermost two current meters were located in the upper isothermal layer (Fig. 2). A current meter was placed at the top of the seasonal thermocline and the fourth current meter was located near the bottom of the seasonal thermocline. Thermistors attached to a multi-conductor cable were placed in the mixed layer and in the thermocline region. The meteorological instruments, which were mounted on a Woods Hole type toroidal buoy, consisted of a wind recorder that measured wind speed and direction, and of air temperature and sea surface temperature recorders. Table 1 shows the depths of the instruments and the instrument record-length distribution.

All current measurements were taken with Richardson-type current meters[1] (Richardson *et al.*, 1963). The sampling scheme consisted of a burst of six samples recorded every 3.75 min; each of the six samples, which consisted of speed, compass and vane, was measured at 5-sec intervals. Between the bursts the instrument was in a "shut-down" mode; current fluctuations with periods between 30 sec and 7.5 min were aliased. The wind recorder, which was a modified Geodyne model A-850 current meter operating in an upside-down position, recorded wind speed and direction with a 3-cup anemometer and a balance wind vane and with the same sampling rate as the current meters. We used a Yellow Springs model 403 thermistor for each of the temperature sensors, and each thermistor was inserted into a nylon slug to increase its time constant to about 6.5 min. The sampling rate of the group of eight thermistors

TABLE 1. Height and depth of the sensors and the instrument record-length distribution. Depth is given for the bottom of the current meter. The start of the experiment was defined as 0800 GMT 4 August 1971, which was 7 hr 44 min after the anchor was released at the sea surface. The end of the experiment occurred at 0800 GMT 5 September 1971, which was 8 hr 25 min before the acoustic release was fired to separate the anchor from the mooring cable.

Instrument	Depth or height (m)	Record length (days)
Wind recorder	2.0	32.0
Air thermistor	1.5	17.5
Surface (water) thermistor	0.4	17.5
Current meter 0285	8.3	32.0
Thermistor 1	9.6	31.4
Current meter 0286	15.8	27.2
Thermistor 2	17.6	5.3
Thermistor 3	23.4	31.4
Current meter 0287	26.2	32.0
Thermistor 4	29.8	31.4
Thermistor 5	36.0	31.4
Thermistor 6	42.1	31.4
Current meter 0288	46.2	32.0
Thermistor 7	48.1	31.4
Thermistor 8	54.2	31.4

[1] Geodyne model A-850-2, manufactured by EG & G Corporation, Waltham, Mass.

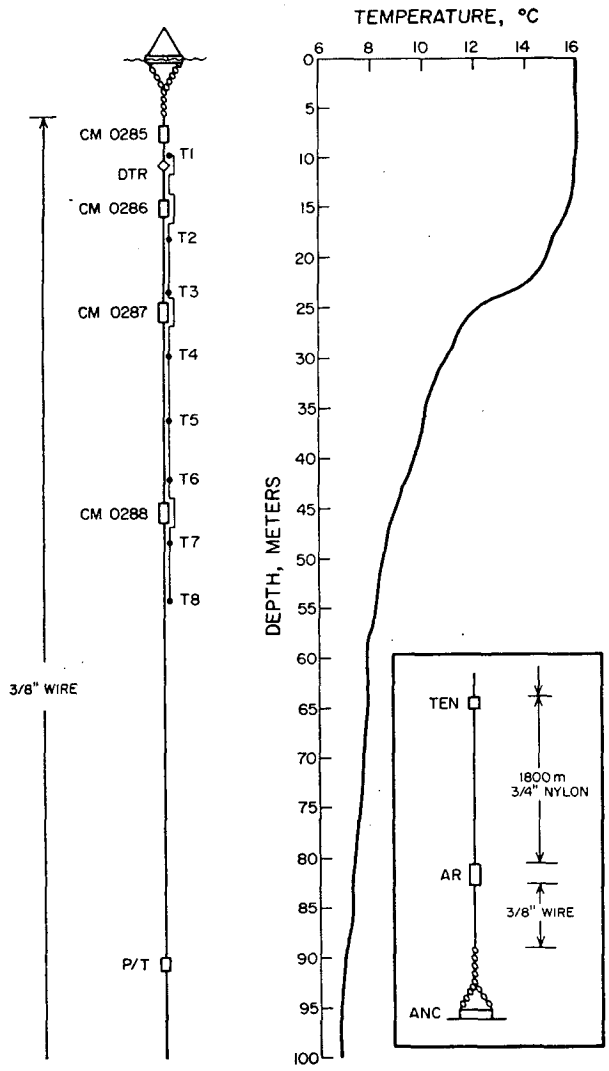

FIG. 2. Positions of the subsurface instruments and the vertical distribution of temperature measured on 3 August 1971 at a site located approximately 23 km northeast of the buoy site: CM = current meter, T1, ..., T8 = thermistors, DTR = digital temperature recorder, P/T = pressure and temperature recorder.

recorded by the Geodyne model A-775 underwater data logger (described by Perry and Smith, 1965) was 5 min.

A recent study (Gould, 1972) showed that current meter measurements made at depths >500 m from beneath a surface buoy moored in deep water contained energy levels that were higher at all frequencies than measurements made beneath a subsurface float. However, Pollard (1973a) and Halpern *et al.* (1974) provide evidence that reliable near-surface current measurements can be made from surface floats. Although the surface-following feature of the surface float would cause the recorded mean motion to be higher than would be measured if surface waves were not present (Pollard, 1973b), this phenomenon does not affect the motion at the inertial frequency. Since the horizontal distribution of temperature was relatively flat, the noise in the temperature measurements produced by the buoy moving around its excursion circle (maximum radius ~1.3 km) would be small. Because the diameter of an excursion circle of a nearly taut elastic mooring is about the same size as the diameter of an inertia circle in mid-latitudes, we assume that in this experiment the magnitude of buoy-induced inertial motion occurring in our measurements was small because of the large vertical shear observed at the inertial frequency between the top and bottom current meters; otherwise, the upper current meter was revolving horizontally in space relative to the position of the anchor while the lower instrument remained fixed.

3. Observations

Summaries of the wind recorder, current meter, and thermistor chain measurements have been presented (Halpern, 1972) as standard statistics, histograms, progressive vector diagrams, time series plots and spectra.

The average 15-min vector-averaged value of the wind speed measured between 4 August and 5 September was about 5.5 m sec^{-1} with a standard deviation of 2.4 m sec^{-1}; the maximum 15-min vector-averaged wind speed (14 m sec^{-1}) was recorded on 20 August. During the experimental period two cold fronts of moderate intensity occurred; the first one passed the buoy site between 1800 GMT 19 August and 0000 on 20 August (Fig. 3) and the other on or about 1 September. As shown in Fig. 4 the wind speeds increased steadily at the rate of about 1.5 m sec^{-1} per day from light breezes on 15 August to strong gusts on 20 August. Wind speeds then dropped rapidly becoming fairly uniform at 5–6 m sec^{-1} between 21 and 28 August when light breezes occurred again. The high winds on 20 August occurred as a transient lasting a short time; we defined the period of the storm as the 9-hr interval centered on 1930 of the 20th when the hourly vector-averaged values of the wind speed were greater than 10 m sec^{-1}. During the storm the wind speeds and directions were quite steady, e.g., the mean and standard deviation of the hourly east speeds, hourly north speeds and hourly vector-averaged speeds were (-0.2 ± 1.8), (11.6 ± 0.9) and (11.8 ± 0.8) m sec^{-1}, respectively.

As shown in Fig. 5 the vertical temperature profiles were significantly altered between 19 and 21 August; a similar change did not occur for the 1 September front passage. The 20 August event produced a more homogeneous temperature distribution above 20 m with the result that the depth of the mixed layer increased from about 18 m to about 25 m. The 6 m spacing between the temperature sensors and the poor data recovery associated with the sensor at 18 m prevent an accurate description of the changes in the vertical distribution of temperature. Above 10 m the temperature decreased and below 20 m the temperatures increased (Table 2); however, the low-frequency variations (i.e., periods

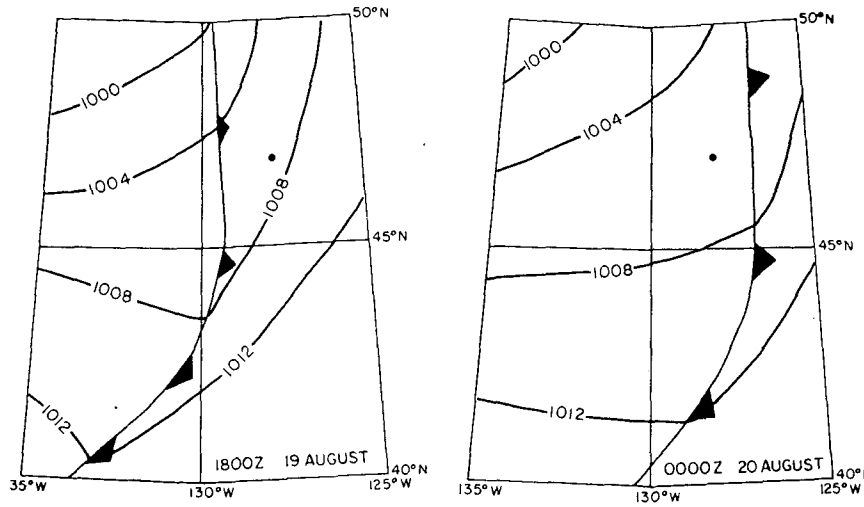

FIG. 3. Sea level atmospheric pressure charts prepared from NOAA's National Weather Service charts.

greater than 12 hr) of the heat content of the water column above 42 m were small and to within ±5% the heat content was undisturbed by the passage of the storm (Fig. 6). Superimposed on the mean value of the heat content were large (20–30%) variations associated with periods of 1 to 12 hr.

Since the heat content of the upper layer changed little when the mixed layer deepened, the redistribution of heat was primarily caused by vertical mixing. If horizontal advection produced the 2C change in temperature at 23 m between 19 and 21 August, then currents of about 2 m sec^{-1} would be expected because the typical horizontal surface temperature gradient in

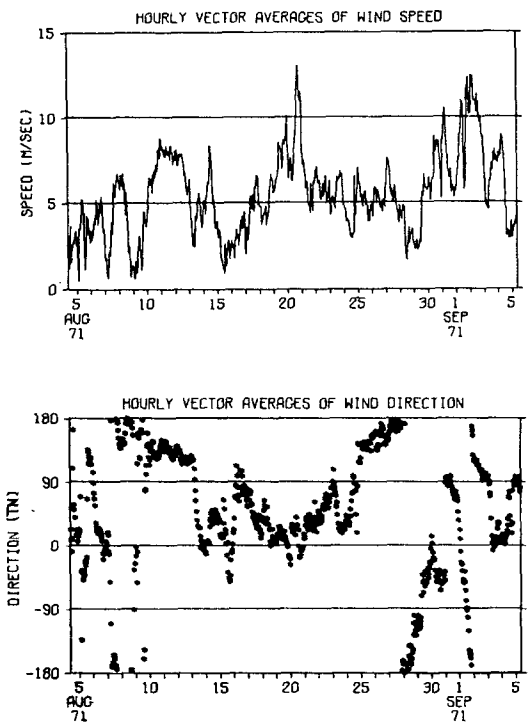

FIG. 4. Time plots of hourly vector averages of wind speed and direction. Wind direction is given as the direction in which the wind is blowing.

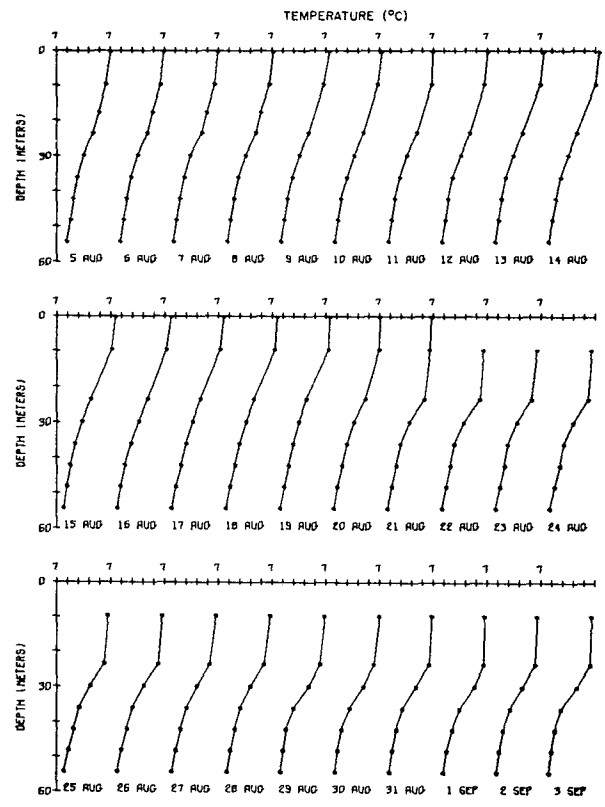

FIG. 5. Vertical profiles of daily mean temperature computed from thermistor measurements. Each tic mark on the abscissa represents 2C; the range of the abscissa for each curve is 7 to 17C with the 7C value superposed upon the 17C value.

TABLE 2. Average daily temperature values before (19 August) and after (21 August) the 20 August storm. The average resolution between each of the thermistors was about 0.08C.

Depth (m)	Temperature (°C) 19 August	21 August	Difference (°C)
0.4	17.73	16.71	−1.02
8.3	17.59	16.49	−1.10
23.4	13.41	15.49	+2.08
29.8	11.99	12.60	+0.61
36.0	10.96	10.98	+0.02
42.1	10.07	10.12	+0.05
48.1	9.26	9.32	+0.06
54.2	8.58	8.58	0.0

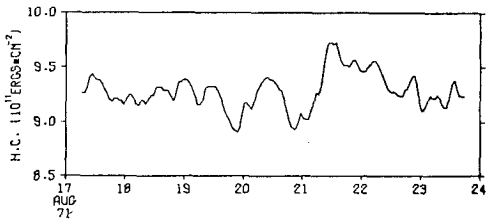

FIG. 6. Thirteen-hour running mean values of the heat content above 42 m [$=\rho_0 c_p \Sigma T_i \Delta z_i$, where ρ_0 is density (1.025 gm cm^{-3}), c_p the heat capacity at constant pressure (4.015 J gm^{-1}), and T_i the temperature corresponding to the depth interval Δz_i].

the northeast Pacific was 0.5C (100 km)$^{-1}$ (Sverdrup *et al.*, 1942: plate 3). Because hourly averages of the air temperature were always slightly greater than the sea surface temperature, the lowering of the surface temperature by static instabilities formed at the sea surface by atmospheric cooling (including nighttime convection) was only remotely significant. According to the reports of the National Weather Service, rain accompanied the storm; thus, free convection by an excess of evaporation over precipitation was not a likely occurrence.

The vector-averaged mean motions computed for the period 5–31 August are given in Table 3. At each depth the temporal variability of the 15-min vector-averaged east and north components, as indicated by the standard deviations, were about equal and were large relative to the mean values. Within the upper 50 m the average current direction was toward the southeast. The 26-day averaged vertical shear was about 1.25 cm sec^{-1} between 8 and 46 m, i.e., the *mean* flow within the upper 50 m was nearly independent of depth. During the 26-day interval the water in the upper 50 m was, on the average, dynamically stable as measured by the Richardson number. Because of the small velocity shear between 26.2 and 46.2 m, the dynamic stability was largest in the stratified water beneath the mixed layer (Table 3).

The words "dynamic stability" and "Richardson number" have been used with a number of different meanings. Miles (1961) and Howard (1961) proved that stability of infinitesimal perturbations in a steady, non-dissipative, stably-stratified shear flow is assured if the *local* Richardson number of the mean flow everywhere exceeds $\frac{1}{4}$. The local Richardson number is defined by $-g\rho^1/(\rho U^{1^2})$, where g is gravity, ρ and ρ^1 are the density and vertical gradient of density, U^1 is the vertical gradient of the mean flow, and the vertical coordinate is positive upward. Instability does not necessarily occur if the local Richardson number is less than $\frac{1}{4}$; furthermore, turbulence may exist when the Richardson number is greater than $\frac{1}{4}$. Munk (1966) and Phillips (1966) have indicated that the Miles-Howard stability criterion is relevant for shearing motion induced by tidal internal waves; presumably a similar argument would be valid for the shear produced by inertial-period motion. In this paper a Richardson number equal to unity defines the condition of marginal stability, i.e., a tendency for a dynamic instability to occur exists, and a Richardson number of $\frac{1}{4}$ defines a critical condition, i.e., the occurrence of shear instability. Because our current meter and temperature time series measurements were not continuous with depth, a vertically averaged Richardson number was computed, i.e.,

$$\mathrm{Ri}=\frac{-g}{\rho}\frac{\Delta\rho}{\Delta z}\Big/\left[\left(\frac{\Delta U}{\Delta Z}\right)^2+\left(\frac{\Delta V}{\Delta Z}\right)^2\right], \qquad (1)$$

where ΔZ is the spacing between the sensors, ΔU and ΔV are the differences between the vector-averaged east and north component speeds, $\Delta\rho$ is the density difference, and ρ the average density of the layer

TABLE 3. Vector-averaged mean motions computed from the 15-min values between 5 and 31 August 1971; average sigma-t values computed from seven repeated STD casts at 2-hr intervals made on 4 August and on 5 September within 1 km of the buoy site; and average values of the Richardson number (Ri) during the 26-day period.

Depth (m)	U (cm sec^{-1}) Mean	Standard deviation	V (cm sec^{-1}) Mean	Standard deviation	Sigma-t (gm cm^{-3})	Ri
8.3	2.08	12.57	−5.98	13.24	23.35	
						12
15.8	3.28	12.65	−3.62	13.43	23.47	
						357
26.2	2.88	8.97	−4.68	10.50	23.93	
						3400
46.2	2.98	6.78	−4.07	8.57	24.61	

between the sensors. One can assume with reasonable assurance that in the region between the sensors values of the local Richardson number will be both higher and lower than the vertically averaged value.

Superimposed upon the 32-day mean flow were large current fluctuations, especially those recorded after the onset of the 20 August storm. Fig. 7 shows that the daily values of the vector-averaged speed measured in the mixed layer were about 300% larger after the onset of the storm than before the arrival of the storm, though the shear in the mixed layer was weak. In contrast to the response of the currents in the mixed layer, the daily averaged values of the currents at 46 m showed little change during the passage of the storm. The vector-averaged hourly values of the east and north components (shown in Halpern, 1972) contained features similar to the ones displayed in Fig. 7; however, on about 22 August the hourly currents at 46 m experienced a significant increase in magnitude for a brief interval of about 6 hr. Thus, the response of the horizontal motion in the stratified water to the storm was delayed and of smaller amplitude and duration compared to the response of the currents in the homogeneous water. Rather than advocate inertial-internal gravity waves propagating slowly downward from the bottom of the mixed layer to explain this time delay, which would correspond to a group velocity with a vertical component of less than 10^{-2} cm sec^{-1}, we believe that the time delay was a function of the magnitude of the vertical velocity shear, *viz.* when the vertical shear across the top of the thermocline reached a critical value related to the stratification, the water became dynamically unstable producing vertical mixing and horizontal motions at depth.

Spectral estimates of the horizontal kinetic energy were computed by first estimating the spectra of the east-component series and the north-component series from Cooley-Tukey Fourier transforms using the perfect Daniell frequency window of variable width. For each spectrum the sum over positive frequencies was equal to the total variance. At each frequency band the east and north spectral estimates were combined by taking half the sum of the two to form the horizontal kinetic energy spectrum (Fig. 8). The spectra indicate the occurrence of inertial and semidiurnal oscillations

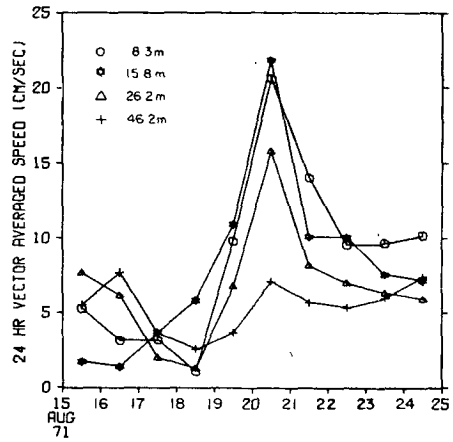

FIG. 7. Daily values of the vector-averaged speed.

statistically significant at the 95% confidence level. At 46.2 m the 95% statistical significance of the inertial peak was marginal; all the other inertial peaks and all the semidiurnal peaks were statistically significant at the 95% confidence level. The rotary spectra (described by Mooers, 1973, and Perkins, 1970) show that the inertial motion was in the clockwise direction and the east and north component spectra show that these oscillations were circularly polarized (Table 4). The vertical shear of the inertial-period motion was about 3.5 times larger than that associated with the semidiurnal tides (Table 4). Within the surface mixed layer the inertial-period motions were coherent and in phase at the 95% confidence level; however, the inertial-period motions measured in the mixed layer and in the stratified water beneath the mixed layer (i.e., between 8 and 46 m) were not coherent (Halpern, 1973). Thus, on the average over the 26-day interval, the inertial-period motion was confined within the upper 50 m.

Unlike barotropic tidal motions which are stationary or quasi-stationary in time, observations of inertial oscillations (Webster, 1968) indicate that they are nonstationary in time. Fig. 9 clearly shows that soon after the time of the onset of the 19 August storm the amplitudes of the inertial oscillations at 8.3 and 15.8 m (i.e., within the surface mixed layer) increased by a factor of about 5; at 26.2 m the amplitude increased

TABLE 4. Kinetic energy spectral estimates associated with the inertial and semidiurnal frequencies. Clockwise and counterclockwise components of the rotary spectra at the inertial frequency are shown. Duration of data = 26 days; $\Delta t = 0.25$ hr; spectral bandwidth at the inertial or semidiurnal frequencies = 4.81×10^{-3} cph; 12 degrees of freedom per estimate. East and north component spectral estimates (6 degrees of freedom) at the inertial frequency are presented.

Depth (m)	Kinetic energy spectra (cm^2 sec^{-2})		Inertial (cm^2 sec^{-2})		Inertial (cm^2 sec^{-2})	
	Inertial	Semidiurnal	Clockwise	Counter-clockwise	East	North
8.3	7.256	6.728	7.183	0.073	6.211	8.301
15.8	8.683	6.643	8.635	0.048	8.360	9.007
26.2	3.508	4.684	3.470	0.037	3.746	3.269
46.2	1.028	4.181	1.015	0.013	0.947	1.108

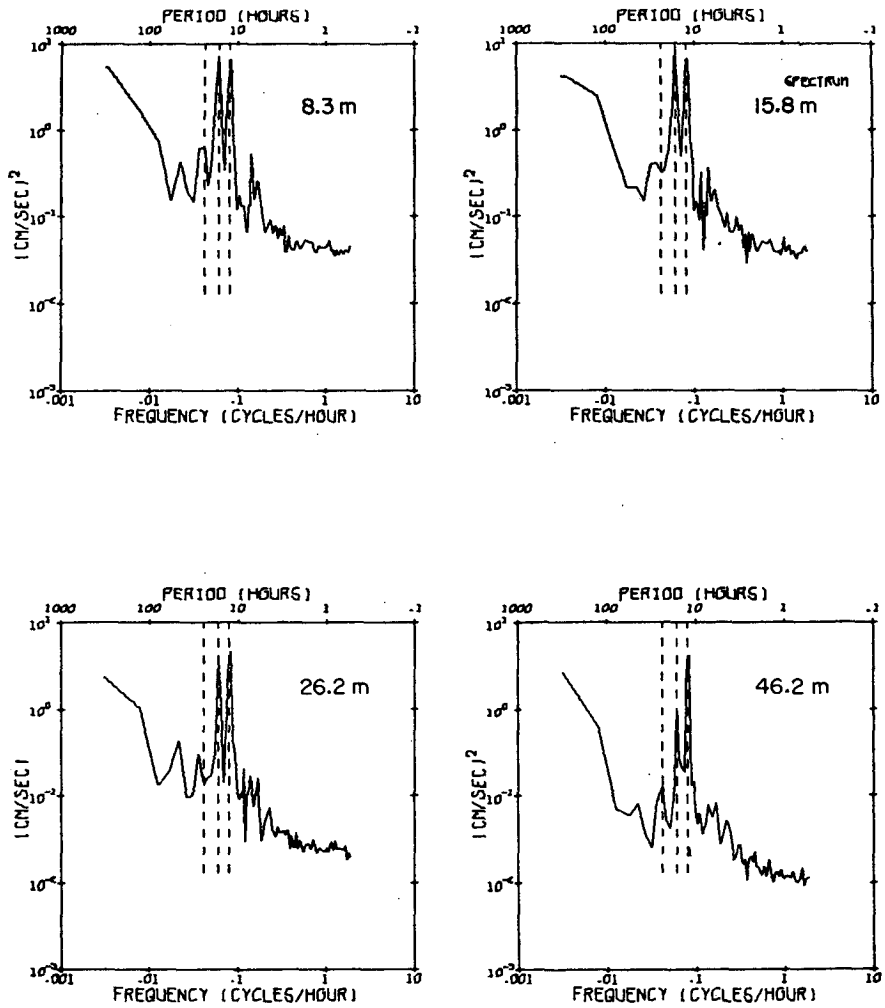

FIG. 8. Horizontal kinetic energy spectra of the velocity fluctuations. For frequencies <0.146 cph (period 6.86 hr) the number of degrees of freedom for each of the kinetic energy spectral estimates was 12, and the 95% confidence limits were equal to 0.514 and 2.726 of each of the estimates. The dashed vertical lines correspond to the diurnal, inertial (0.061 cph) and semidiurnal frequencies.

by a factor of 3.5; and it is evident that the storm did not generate inertial-period motion at 46.2 m (i.e., in the stratified water). At 46 m the increase in the amplitude on 22 August provides some evidence, albeit small, of a response to the storm consistent with the time delay discussed above. As shown in Fig. 9 the response time for the generation of inertial oscillations in the upper ocean was small compared to the inertial period. There was zero phase difference between the inertial oscillations recorded at the upper three current meters, providing evidence that after the arrival of the storm the 25 m thick mixed layer moved as a slab with oscillatory (inertial-period) motion. During the interval 20–23 August the vertical shear associated with the inertial frequency was largest across the transition zone (between 16 and 26 m); moreover, this frequency component of the vertical shear was about 1.6 times larger than the value of the mean current shear, assuming that the inertial oscillations were effectively filtered from the total current by averaging the recorded data over a 3-day period.

Using the basic data sets (i.e., 15-min vector averages of currents and 15-min averages of temperature), 15-min averages of the vertically averaged Richardson number (Ri) were computed for each of the layers between the current meters. Average salinity values were obtained from average vertical profiles computed from seven STD casts made at 2-hr intervals on 4 August and on 5 September. Because the thermistor at 17.6 m was inoperative, the temperature values at 9.6 and 23.6 m were used to compute the Richardson number between 8.3 and 15.8 m and between 15.8 and 26.2 m. Because we had only four current meters, seven thermistors, and no conductivity sensors, the profiles of current and

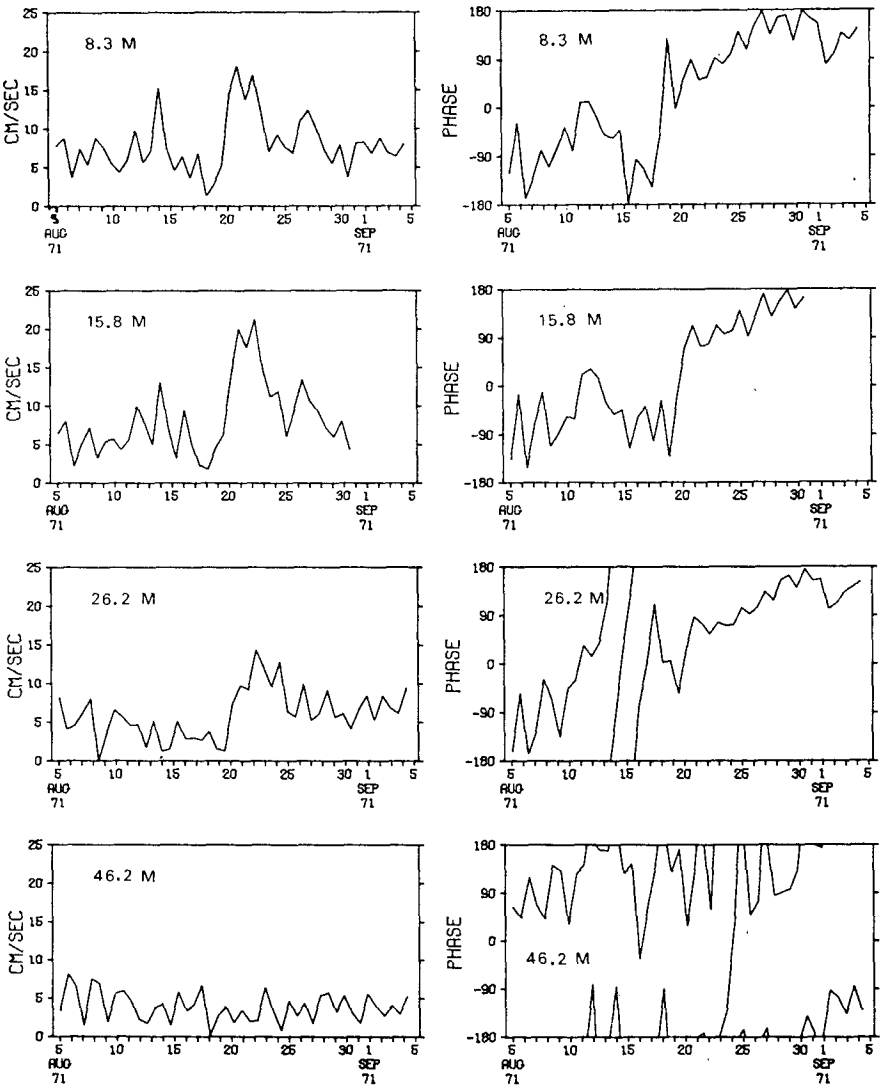

FIG. 9. Temporal variations of the inertial-period motion. Each estimate represents an average value over a time interval equal to two inertial periods; each interval overlapped the previous one by one inertial period. Estimates were computed from the periodogram ordinates.

density used in the computation of Ri were smooth, eliminating any fine-scale structure that would tend to produce even smaller values of the local Richardson number. Fig. 10 shows that for about 7 days after the onset of the 19 August storm, the dynamic stability of the layer between 16 and 26 m was marginal ($\mathrm{Ri}<1$). Because the Brunt-Väisälä frequency used to compute the Richardson number in the upper and middle layers was virtually the same, the temporal variations of Ri between 8 and 26 m were also very similar. Below 26 m the Richardson number indicates that the water was always dynamically stable. Early on 20 August the square of the Brunt-Väisälä frequency decreased by an order of magnitude in the upper region and late on 20 August the shear-squared increased by an order of magnitude in the middle region.

4. Vertical mixing

In a stably stratified shear flow the intensity of vertical mixing, represented by the vertical eddy viscosity coefficient (A_v), is dependent upon both the stratification and the shear, represented by the Richardson number. Because of the scarcity of current observations in the upper region of the ocean the functional relationship between A_v and Ri is very poorly known. Generally the relationship is of the form

$$A_v=A_v^0(1+\sigma\mathrm{Ri})^n, \tag{2}$$

where A_v^0 is the vertical eddy viscosity coefficient for regions of neutral stability (i.e., $\partial\rho/\partial z=0$), and σ and n are constants. We used $\sigma=10$ and $n=-\frac{1}{2}$ (Munk and Anderson, 1948). To compute A_v, we assumed A_v^0

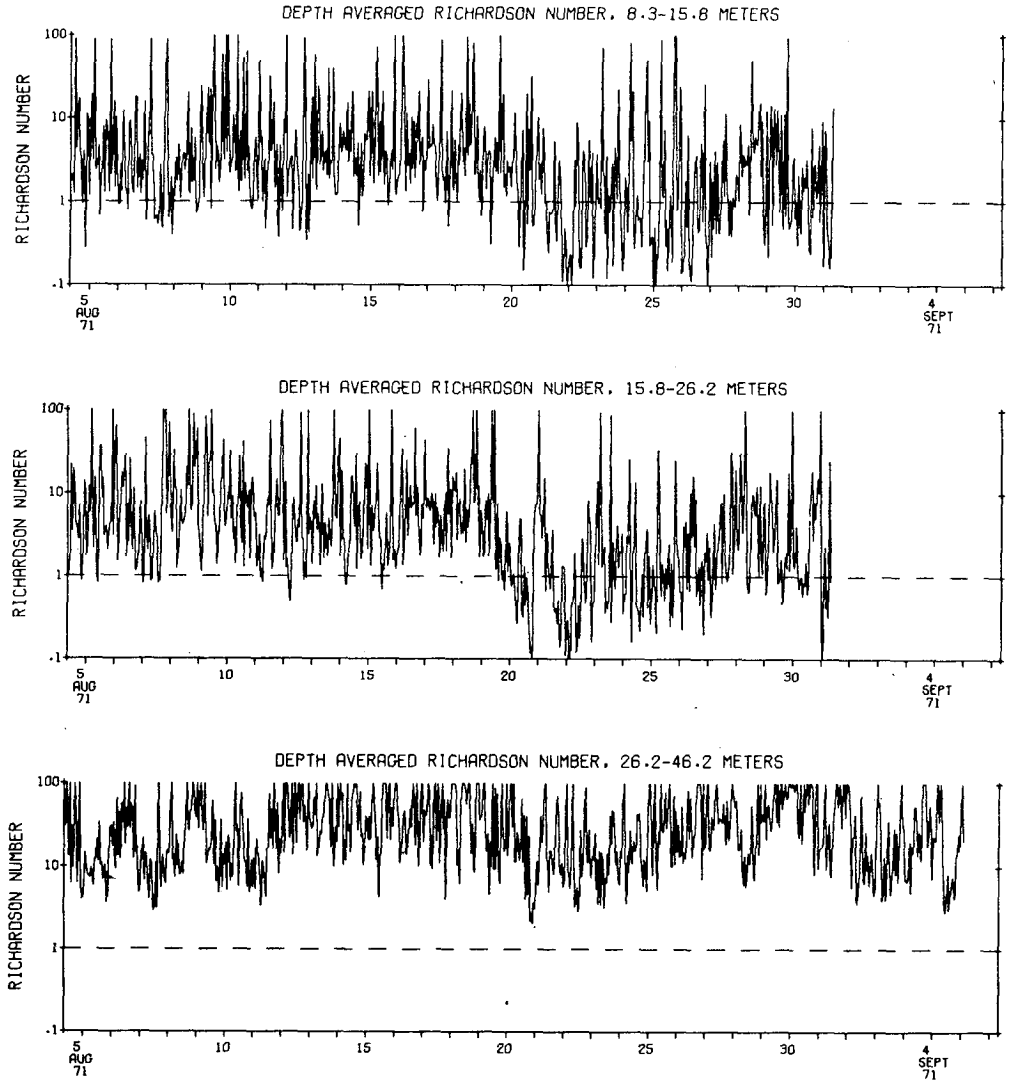

FIG. 10. Fifteen-minute averages of the Richardson number. Values greater than 100 were arbitrarily defined as equal to 100. Dashed horizontal line, which is equal to 1.0, represents the condition for marginal dynamic stability.

was constant throughout the mixed layer and was determined from Ekman's (1905) theory of wind-driven currents in a homogeneous ocean.

The wind stress τ_0 was defined by the bulk areodynamic parameterization

$$\frac{\tau_0}{\rho_a}=u_*^2=C_z W_z^2, \tag{3}$$

where ρ_a, u_*, C_z and W_z represent the density of the air (1.25×10^{-3} gm cm^{-3}), the friction velocity, the drag coefficient, and the mean wind speed, respectively; C_z and W_z are specified for the same height z, and as Pond (1972) indicates, W_z should represent an average speed over one to at most a few hours. The drag coefficient varies with the static stability of the air, but because the potential air temperature and the sea surface temperature were nearly equal the correction would have been insignificant. We referenced our observations to the 10 m level and used $C_{10}=1.3\times10^{-3}$ (Kraus, 1972), which is generally considered to be applicable with an uncertainty of 20% up to wind speeds of about 15 m sec^{-1}. Assuming hydrostatically neutral conditions and the logarithmic wind profile in the constant stress layer, the wind speed at the 10 m level is related to the wind observations made at 2 m above the sea surface by

$$W_{10}-W_2=1.6094\frac{u_*}{\kappa}, \tag{4}$$

where the value of κ, von Kármán's constant, is 0.4, although Businger *et al.* (1971) have suggested $\kappa=0.35$.

Substitution of $u_*=\sqrt{C_{10}}\,W_{10}$ yields

$$W_{10}=1.17\,W_2. \tag{5}$$

The Ekman transport computed from the mean vector-averaged storm wind speed ($W_{10}=13.5$ m sec^{-1}) was equal to approximately 2.8×10^4 gm cm^{-1} sec^{-1}, or about 14 cm sec^{-1} when converted to a mean speed of the water column 0 to 20 m. To compute the mean storm-induced currents we averaged the current measurements over 51 hr to filter the inertial and semidiurnal oscillations. The 51-hr vector-averaged speed and direction of the currents at 8 and 16 m measured on 20 and 21 August were 14 cm sec^{-1}, 145° and 12 cm sec^{-1}, 135°. These directions were about 140° to the right of the mean direction of the storm wind, and about 120° to the right of the vector-averaged mean wind direction computed during the 48-hr interval of 20 and 21 August; the veering angle between the current transport and the wind was not totally inconsistent with Ekman's result. Allowing for an ambient (non wind-generated) current of about 3 cm sec^{-1} (Dodimead *et al.*, 1963), the ratio between the wind-generated current and the computed Ekman current was about 0.7, a value close enough to unity so that our subsequent use of Ekman theory is not totally unfounded.

In an unbounded homogeneous ocean of infinite depth the surface drift current (V_0^E) generated by a uniform wind stress is related to the constant vertical eddy viscosity coefficient (A_v^0) (Ekman, 1905):

$$A_v^0=\frac{\rho_a{}^2C_{10}{}^2}{\rho^2 f}\left(\frac{V_0^E}{W_{10}}\right)^{-2}W_{10}{}^2. \tag{6}$$

The measured wind factor at our experimental site ($\theta=47$N), defined as the ratio between the wind-induced surface current and the storm wind speed (i.e., V_0/W_{10}), was equal to about 0.0074. Our value was about half as large as values determined by Thorade (1914) and Palmén (1931), and about equal to the wind factor measured by Durst (1924). Substitution of $(V_0/W_{10})=0.0074$ for (V_0^E/W_{10}) in (6) yields

$$A_v^0=4.3\times10^{-4}W_{10}{}^2. \tag{7}$$

Thus, our functional relationship between A_v, W_{10} and Ri is

$$A_v=\frac{4.3\times10^{-4}W_{10}{}^2}{(1+10\mathrm{Ri})^{\frac{1}{2}}}. \tag{8}$$

The observations made in the region 16 to 26 m indicate that the large values of the wind speeds (>10 m sec^{-1}) were measured about a day before the simultaneous occurrence of the low Richardson numbers and the vertical redistribution of temperature; therefore, when estimating A_v it seemed appropriate to use the wind speeds measured during the storm with Richardson number values computed at later times. The maximum value of A_v determined from (8) was about 820 cm^2 sec^{-1}; it corresponded to a Richardson number of 0.1 and to the maximum recorded value of the 15-min vector averaged wind speed. Using the mean value of the vector-averaged storm wind speed with the Richardson number (Ri=4.6) computed for the 24-hr interval beginning at noon on 21 August when the dynamic stability in the region 16 to 26 m was very weak, the value of A_v was about 114 cm^2 sec^{-1}. During the 32-day experimental period a typical value of A_v was ~1.0 cm^2 sec^{-1}; this value was computed using a Richardson number of 357 and an alternate form of (6):

$$A_v^0=\frac{\langle\tau_0\rangle^2}{\rho^2V_0^{E2}f},$$

where

$$\left.\begin{aligned}\langle\tau_0\rangle&=(\langle\tau_x\rangle^2+\langle\tau_y\rangle^2)^{\frac{1}{2}}\\(\tau_x,\tau_y)&=\rho_aC_{10}(|\mathbf{u}|u,\ |\mathbf{u}|v)\end{aligned}\right\},$$

(u, v) represent hourly averages of the east and north wind speeds, the angle brackets denote a 32-day time-average, and $V_0^E=(\langle u\rangle^2+\langle v\rangle^2)^{\frac{1}{2}}=3$ cm sec^{-1} (Halpern, 1972). The large difference between the long- and short-period mean values of A_v resulted because the vertical exchange of water was a transient phenomenon lasting only a few days, with very little mixing occurring during the remainder of the 32-day experimental period.

In the region from 26 to 46 m where the stratification increased after the onset of the storm, the Richardson number was always greater than unity and its distribution with time was fairly uniform (Fig. 9). Using a mean Richardson number of about 115 for the 24-hr interval cenered on 0000 (22 August), the value of A_v was about 25 cm^2 sec^{-1}, about one-fifth the value determined for the region above it.

Our values of A_v are compared with the relatively few estimates determined from direct current measurements made near the surface and reported elsewhere. Jones (1973) computed values of A_v in the Equatorial Undercurrent using the logarithmic profile to form a functional relation between A_v and Ri that was independent of the wind speed; for a mean value of Ri=0.8, the mean value of A_v between 40 and 20 m was about 39 cm^2 sec^{-1}. Smith (1973) estimated A_v in the mixed layer under the Arctic ice after the passage of a storm from current meter measurements of the Reynolds stresses; between 4 and 20 m the mean value of Ri was about 100 and A_v was about 40 cm^2 sec^{-1}. Smith (1973) reports that the mixed layer may have been produced by free convection. Hunkins (1966), using tethered drogues to measure currents under the Arctic ice, found a well-developed Ekman spiral averaged over a 10-day meteorologically quiet interval ($W\approx4$ m sec^{-1}); the 18 m frictional depth, which was less than the thickness of the mixed layer, was equivalent to $A_v=24$ cm^2 sec^{-1}. To the author's knowledge,

there are no estimates of A_v made under conditions similar to our own.

The rate of working by the wind stress at 10 m height is given by (Kraus, 1972)

$$E_a=\tau_0 W_{10}=\rho_a C_{10} W_{10}^3. \quad (9)$$

According to Kraus and Turner (1967) the turbulent energy available for mixing is produced at a rate that is some constant fraction m of the rate of downward transfer of turbulent energy from the wind field, *viz.* the available mixing energy is mE_a. Using Turner's (1969) method, we estimated m from the hourly averages of the vertical distributions of temperature. Assuming that the salinity did not contribute significantly to the density structure, the potential energy was defined by

$$\mathrm{PE}=\rho g\alpha\int_0^{z_0}(T-T_{z_0})z\,dz, \quad (10)$$

where α is the coefficient of thermal expansion $[2\times10^{-4}(°\mathrm{C})^{-1}]$, T is the temperature at depth z, and T_{z_0} the reference temperature at z_0 that is unaffected by surface processes.

The natural variability of oceanographic and meteorological conditions makes the determination of m within narrow limits very difficult, e.g., the relevant time between the passage of the storm and the occurrence of mixing is imprecisely known because of the non-uniform wind speeds and directions and because of the temporal variations of the vertical distribution of temperature caused by internal gravity wave motions. A typical value of the potential energy between 0 and 42 m was about 7×10^6 ergs cm^{-2}. Successive values of the hourly averages of PE varied by about $\pm15\%$ (Fig. 11), which is not too surprising since the spectra of the temperature measurements showed a large amount of thermal activity, especially at the semidiurnal frequency (Halpern, 1972). Assuming that all the spectral energy recorded in the temperature measurements in the 6.65×10^{-2} cycle per hour (cph) frequency band centered on the M_2 frequency was due to internal wave motion, an upper bound of the semidiurnal internal wave potential energy occurring between 25 and 45 m would be approximately 5×10^3 ergs cm^{-2}, a value much too small to account for the fluctuations in the PE estimates. Because the temperature variations below 48 m were quite small, we used (10) to compute the PE of the semi-diurnal temperature variations occurring between 25 and 45 m; the magnitude was about 1×10^6 ergs cm^{-2}, or about 15% of the mean value. Thus, although the energy of the internal waves was small, these waves could have produced the observed short-period fluctuations of the potential energy. For these reasons we filtered the hourly averages of the potential energy time series with a 13-hr running mean.

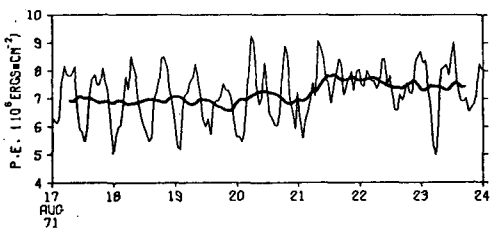

FIG. 11. Hourly averaged values (light curve) and 13-hr running mean values (heavy curve) of the potential energy for depths above 42 m.

Before the arrival of the storm the average value of the 13-hr running mean values of the potential energy of the uppermost 42 m was relatively constant from one day to the next; during 18 August the average value of the potential energy was 6.92×10^6 ergs cm^{-2}. Early on the 21st the 13-hr running means increased in magnitude until about 1000 on 21 August when they again became relatively constant; during the 24-hr interval beginning at 1000 on 21 August the average value of the potential energy was about 7.73×10^6 ergs cm^{-2}. If the onset time of the storm is defined as the 9-hr interval centered at 1930 on 20 August, then the time rate of change of the potential energy over the 14.5-hr interval was about 15.5 ergs cm^{-2} sec^{-1}. Thus, m was equal to 0.0039. This estimate of m was about 2.5 times smaller than the one determined by Turner (1969) and about 3 times larger than the one determined by Denman (1973b), although it was only slightly greater than the upper limit of the range of m values measured by Denman.

5. Discussion

The observations made at our buoy site in the northeast Pacific indicate that during undisturbed atmospheric conditions when the vector-averaged mean wind speed was about 5 m sec^{-1}, the depth of the surface mixed layer remained constant, the velocity shear within the upper 50 m was small, and the transition zone between the mixed layer and the stratified water beneath it was dynamically stable (as measured by the Richardson number). When a cold front accompanied by wind speeds of 10–14 m sec^{-1} passed the buoy site early on 20 August, the vertical distribution of temperature was significantly altered and the depth of the mixed layer increased from about 18 m to about 25 m. The heat content of the upper region was little changed by the storm. Free convection was not a likely occurrence and the forced convection can be regarded as one-dimensional because disturbances due to advection were quite small. Within a half-pendulum day after the onset of the storm, large currents, especially at the inertial frequency, were measured in the mixed layer; yet the motions within the stratified water beneath the mixed layer were only weakly coupled to the large rapid increase in the wind stress. The increase in the current shear across the transition zone apparently

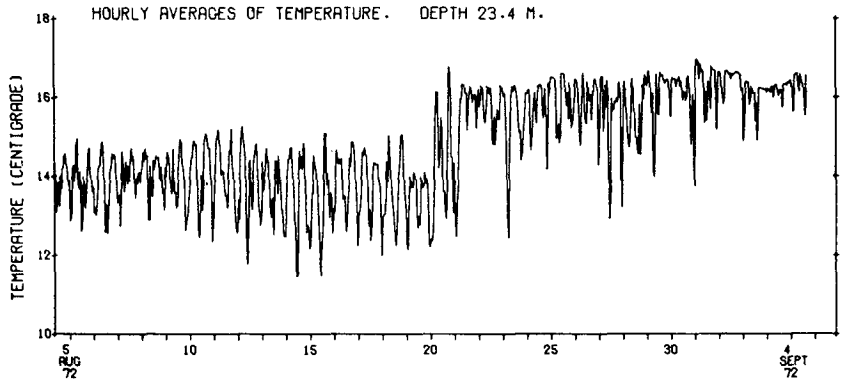

FIG. 12. Hourly averages of temperature at a depth of 23.4 m.

was large enough to decrease the dynamic stability below the condition of marginal stability so that vertical mixing occurred; the depth-averaged Richardson number between 16 and 26 m dropped below unity for a span of a few days and during this period many hourly averaged values of the Richardson number were less than $\frac{1}{4}$. Presumably the mixing was produced by small-amplitude internal perturbations (e.g., ubiquitous internal gravity shear wave motions in the seasonal thermocline duct) that grew in size by extracting energy from the wind-induced current shear. Evidence of the vertical redistribution of temperature in the stratified water underlying the surface mixed layer was the abrupt 2C increase in the quasi-mean temperature at 23 m (Fig. 12) that occurred on 20–21 August; this temperature change coincided with the time when the Richardson number dropped below unity.

Quantitative estimates of the intensity of vertical mixing were made from a derived functional relation between the wind speed, the Richardson number, and the vertical eddy viscosity coefficient. In the region from 16 to 26 m the maximum value of A_v was about 800 cm^2 sec^{-1}; a 24-hr mean value occurring during the time of mixing was 114 cm^2 sec^{-1} and a typical value associated with the generally quiescent 32-day period was 1.0 cm^2 sec^{-1}. From 26 to 46 m where little vertical mixing was observed the 24-hr mean value of A_v associated with the time of mixing was about 25 cm^2 sec^{-1}. These values represent depth averages; local values would presumably be larger. The empirical determination of the wind factor from only one set of coordinates and the many assumptions used in the expression relating W_{10}, Ri and A_v surely lead one to suspect our estimates of A_v, at least until additional independent estimates are determined.

Approximately one-half pendulum day after the time of arrival of the storm, the vertical current shear increased and the Richardson number decreased in the region between 16 and 26 m, and the potential energy of the water column above 42 m increased. Because the arrival time of the storm was ill-defined, the relevant time between the time of increase in the wind speed and the time of the onset of mixing was also poorly defined. Assuming the storm began when the 15-min vector-averaged wind speeds became larger than 10 m sec^{-1}, then $m=0.003$ (relevant time=19 hr), or $m=0.004$ when the onset time of the storm was equal to the middle of the 9-hr period of high winds. Thus, about 0.3–0.4% of the kinetic energy input of the wind field to the water was available for vertical mixing.

The temperature data, although limited in vertical extent, indicated that the depth of the mixed layer increased from about 18 m to about 25 m on 20 August. This is consistent with the results reported by Tabata *et al.* (1965) who determined a linear relationship between the depth of the summer surface mixed layer and wind speed using bathythermograph data at Ocean Station "P", e.g., an average wind speed over 12 hr of 10 m sec^{-1} would correspond to a mixed layer depth of (18±6) m. Because current meter measurements were not made they could only speculate that a velocity shear in the region of the seasonal thermocline was a potential source of the forced convection.

In the Pollard *et al.* (1973) theoretical model of the local response of the surface layer of the ocean to a transient wind stress, the criterion for the rapid deepening of the wind-mixed layer was based on the dynamic stability (as measured by the Richardson number) of the stably stratified fluid below the homogeneous layer. Their model predicts that after one-half inertial period the thickness of the mixed layer reached its maximum value given by

$$h_{\max}=1.68\left(\frac{\tau_0}{\rho f N}\right)^{\frac{1}{2}}. \tag{11}$$

For $W_2=11.5$ m sec^{-1} and N (initial Brunt-Väisälä frequency)$=0.023$ rad sec^{-1}, $h_{\max}=18$ m; the fairly good agreement seems remarkable considering the simplicity of the model and the contamination of the observational results by the lack of data. In agreement with their model the vertical distribution of tempera-

ture was not appreciably changed by the passage of the 1 September storm because the wind speeds were less than the ones accompanying the 20 August storm.

Acknowledgments. I thank Dr. Maurice Rattray, Jr., for valuable critiques. I am indebted to James R. Holbrook for his able programming and ability to keep track of endless numbers, and to R. Michael Reynolds for constructing new instruments and modifying old ones.

This near-surface circulation study was supported by the International Decade of Ocean Exploration office of the National Science Foundation under NSF Agreements AG-253 and AG-299, and this support is gratefully acknowledged.

REFERENCES

Businger, J. A., J. C. Wyngaard, Y. Izumi and E. F. Bradley, 1971: Flux profile relationships in the atmospheric surface layer. *J. Atmos. Sci.*, **28**, 181–189.

Denman, K. L., 1973a: A time-dependent model of the upper ocean. *J. Phys. Oceanogr.*, **3**, 173–184.

——, 1973b: Energy changes associated with wind mixing in the upper ocean. Tech. Rept. 380, Fish. Res. Bd. Can., 15 pp.

Dodimead, A. J., F. Favorite and T. Hirano, 1963: Review of oceanography of the subarctic Pacific region. *Bull. North Pac. Fish. Comm.*, **13**, 1–500.

Durst, C. S., 1924: The relationship between current and wind. *Quart. J. Roy. Meteor. Soc.*, **50**, 113.

Ekman, V. W., 1905: On the influence of the earth's rotation on ocean currents. *Ark. Mat. Astron. Fys.*, **2**, No. 11.

Gould, J., 1972: SCOR moorings, some preliminary results. MODE Hot-Line News, No. 16 (unpublished results).

Halpern, D., 1972: Wind recorder, current meter and thermistor chain measurements in the northeast Pacific, August/September 1971. NOAA Tech. Rept. ERL 240-POL 12, 37 pp.

——, 1973: On the estimation of a complex-valued coherency function using discrete Fourier transform. *Preprints Third Conf. Probability and Statistics in Atmospheric Science*, 19–22 June, Boulder, Colo., Amer. Meteor. Soc., 157–164.

——, R. D. Pillsbury and R. L. Smith, 1974: An intercomparison of three current meters in shallow water. *Deep Sea Res.* (in press).

Howard, L. N., 1961: Note on a paper by John W. Miles. *J. Fluid Mech.*, **10**, 509–512.

Hunkins, K., 1966: Ekman drift currents in the Arctic Ocean. *Deep Sea Res.*, **13**, 607–620.

Jones, J. A., 1973: Vertical mixing in the Equatorial Undercurrent. *J. Phys. Oceangr.*, **3**, 286–296.

Kraus, E. B., 1972: *Atmosphere-Ocean Interaction*. Oxford, Clarendon Press, 271 pp.

——, and J. S. Turner, 1967: A one-dimensional model of the seasonal thermocline. II, The general theory and its consequences. *Tellus*, **19**, 98–106.

Miles, J. W., 1961: On the stability of heterogeneous shear flows. *J. Fluid Mech.*, **10**, 496–508.

Mooers, C. N. K., 1973: A technique for the cross spectrum analysis of pairs of complex-valued time series, with emphasis on properties of polarized components and rotational invariants. *Deep Sea Res.* (in press).

Munk, W. H., 1966: Abyssal recipes. *Deep Sea Res.*, **13**, 707–730.

——, and E. R. Anderson, 1948: Notes on a theory of the thermocline. *J. Marine Res.*, **7**, 276–295.

Niiler, P., 1973: Deepening of the wind-mixed layer. (Unpublished manuscript.)

Palmén, E., 1931: Zur Bestimmung des Triftstromes aus Terminbeobachtungen. *J. Conseil Intern. Explor. Mer.*, **6**, 387–401.

Perkins, H. T., 1970: Inertial oscillations in the Mediterranean. Ph.D. thesis, Massachusetts Institute of Technology, Cambridge.

Perry, K. E., and P. F. Smith, 1965: Digital methods of handling oceanographic transducers. *Marine Sciences Instrumentation*, Vol. 3. New York, Plenum, 25–39.

Phillips, O. M., 1966: *The Dynamics of the Upper Ocean*. Cambridge University Press, 261 pp.

Pollard, R. T., 1970: On the generation by winds of inertial waves in the ocean. *Deep Sea Res.*, **17**, 795–812.

——, 1973a: The Joint Air-Sea Interaction Trial-JASIN 1972. *Proc. Fifth Liege Colloquium on Ocean Hydrodynamics*, Soc. Roy. Sci. Liege (in press).

——, 1973b: Interpretation of near-surface current meter observations. *Deep Sea Res.*, **20**, 261–268.

——, and R. C. Millard, Jr., 1970: Comparisons between observed and simulated wind-generated inertial oscillations. *Deep Sea Res.*, **17**, 813–821.

——, P. B. Rhines and R. O. R. Y. Thompson, 1973: The deepening of the wind-mixed layer. *Geophys. Fluid Dyn.*, **4**, 381–404.

Pond, S., 1972: The exchanges of momentum, heat and moisture at the ocean-atmosphere interface. *Proc. Conf. Numerical Models of Ocean Circulation*, Durham, N. H., Nat. Acad. Sci. (in press).

Richardson, W. S., P. B. Stimson and C. H. Wilkins, 1963: Current measurements from moored buoys. *Deep Sea Res.*, **10**, 369–388.

Sakou, T., 1970: Inertial period oscillation in response to local atmospheric motion. *La Mer*, **8**, 235–240.

Smith, J. D., 1973: Turbulent structure of the surface boundary layer in an ice-covered ocean. *Proc. 1972 ICES Symp. Physical Processes for the Dispersal of Pollutants in the Sea* (in press).

Sverdrup, H. U., M. W. Johnson and R. H. Fleming, 1942: *The Oceans*. New Jersey, Prentice-Hall, 1087 pp.

Tabata, S., N. E. J. Boston and F. M. Boyce, 1965: The relation between wind speed and summer isothermal surface layer of water at Ocean Station "P" in the eastern subarctic Pacific Ocean. *J. Geophys. Res.*, **70**, 3867–3878.

Thorade, H., 1914: Die Geschwindigkeit von Triftstromungen. *Wiss. Beil., Realschule zu Eilbeck*, 1913–1914.

Turner, J. S., 1969: A note on wind mixing at the seasonal thermocline. *Deep Sea Res.*, **16** Suppl., 297–300.

Uda, M., 1963: Oceanography of the subarctic Pacific Ocean. *J. Fish. Res. Bd. Can.*, **20**, 119–179.

Webster, F., 1968: Observations of inertial-period motions in the sea. *Rev. Geophys.*, **6**, 473–490.

——, 1972: Estimates of the coherence of ocean currents over vertical distances. *Deep Sea Res.*, **19**, 35–44.